Chemistry & Biology
Article

Chemical Knockout of Pantothenate Kinase Reveals the Metabolic and Genetic Program Responsible for Hepatic Coenzyme A Homeostasis

Yong-Mei Zhang,[1] Shigeru Chohnan,[1,4] Kristopher G. Virga,[2] Robert D. Stevens,[3] Olga R. Ilkayeva,[3] Brett R. Wenner,[3] James R. Bain,[3] Christopher B. Newgard,[3] Richard E. Lee,[2] Charles O. Rock,[1] and Suzanne Jackowski[1,*]

[1] Department of Infectious Diseases, St. Jude Children's Research Hospital, Memphis, TN 38105, USA
[2] Department of Pharmaceutical Sciences, University of Tennessee Health Science Center, Memphis, TN 38163, USA
[3] Sarah W. Stedman Nutrition and Metabolism Center, Duke University Medical Center, Durham, NC 27704, USA
[4] Present address: Department of Bioresource Science, College of Agriculture, Ibaraki University, Ibaraki 300-0393, Japan.
*Correspondence: suzanne.jackowski@stjude.org
DOI 10.1016/j.chembiol.2007.01.013

SUMMARY

Coenzyme A (CoA) is the major acyl group carrier in intermediary metabolism. Hopantenate (HoPan), a competitive inhibitor of the pantothenate kinases, was used to chemically antagonize CoA biosynthesis. HoPan dramatically reduced liver CoA and mice developed severe hypoglycemia. Insulin was reduced, glucagon and corticosterone were elevated, and fasting accelerated hypoglycemia. Metabolic profiling revealed a large increase in acylcarnitines, illustrating the role of carnitine in buffering acyl groups to maintain the nonesterified CoASH level. HoPan triggered significant changes in hepatic gene expression that substantially increased the thioesterases, which liberate CoASH from acyl-CoA, and increased pyruvate dehydrogenase kinase 1, which prevents the conversion of CoASH to acetyl-CoA. These results identify the metabolic rearrangements that maintain the CoASH pool which is critical to mitochondrial functions, including gluconeogenesis, fatty acid oxidation, and the tricarboxylic acid and urea cycles.

INTRODUCTION

Coenzyme A (CoA) is an essential cofactor that carries carboxylic acid substrates and supports a multitude of oxidative and synthetic metabolic reactions, including those involved in the citric acid cycle, sterol biosynthesis, amino acid metabolism, and fatty acid biosynthesis and oxidation [1]. CoA is derived from vitamin B_5 (pantothenate), cysteine, and ATP. Pantothenate kinase (PanK) catalyzes the first committed step and is the rate-controlling enzyme in CoA biosynthesis [1–3]. PanK expression levels define the upper threshold of the cellular CoA content [4–6], and PanK biochemical activities are feedback regulated differentially by nonesterified CoA (CoASH) or CoA thioesters [4, 6–10], providing a mechanism to coordinate the rate of CoA synthesis with the demand for the cofactor in metabolic pathways. Loss of the feedback regulation by mutation at a single PanK residue results in runaway CoA production [11].

The discovery of multiple PanK isoforms encoded by four genes in humans [12–16] and mice [7] suggests a complexity associated with diet-, drug-, and disease-induced responses of the PanK activities which, in turn, regulate CoA availability. Liver CoA levels are apparently important in metabolic function, as hepatic total PanK activity and CoA content are altered in response to nutritional state [17–21], insulin [3], glucagon or glucocorticoids [18], fibrate drugs [17, 22–25], and diabetes [26, 27]. The human PanK2 is a mitochondrial isoform [14, 28, 29] that is sensitive to inhibition by submicromolar acetyl-CoA [16], and mutations that inactivate this isoform are associated with a neurodegenerative disorder [12, 14, 28, 29]. Loss of one or more of the PanKs would presumably lead to chronically reduced tissue CoA levels, but details about the molecular sequelae that accompany such a disorder are lacking. We investigated the biochemical and genetic alterations imposed on animals by reduced CoA using a pantothenate antimetabolite, hopantenate (HoPan; Figure 1A) to chemically ablate CoA biosynthesis. The data show that nonesterified CoASH is the most important component of the CoA pool that is necessary for mitochondrial function. The experiments also illustrate the metabolic and genetic processes that realign in an effort to maintain the level of CoASH. These data provide insight into the molecular shifts that may contribute to a loss of physiological function due to CoA deficiency.

RESULTS

Biochemistry of HoPan Action

HoPan is a structural analog of pantothenate containing an extra methylene group (Figure 1A), and we identified this molecule as a pantothenate kinase inhibitor as part of an enzyme-based screen of pantothenamides and

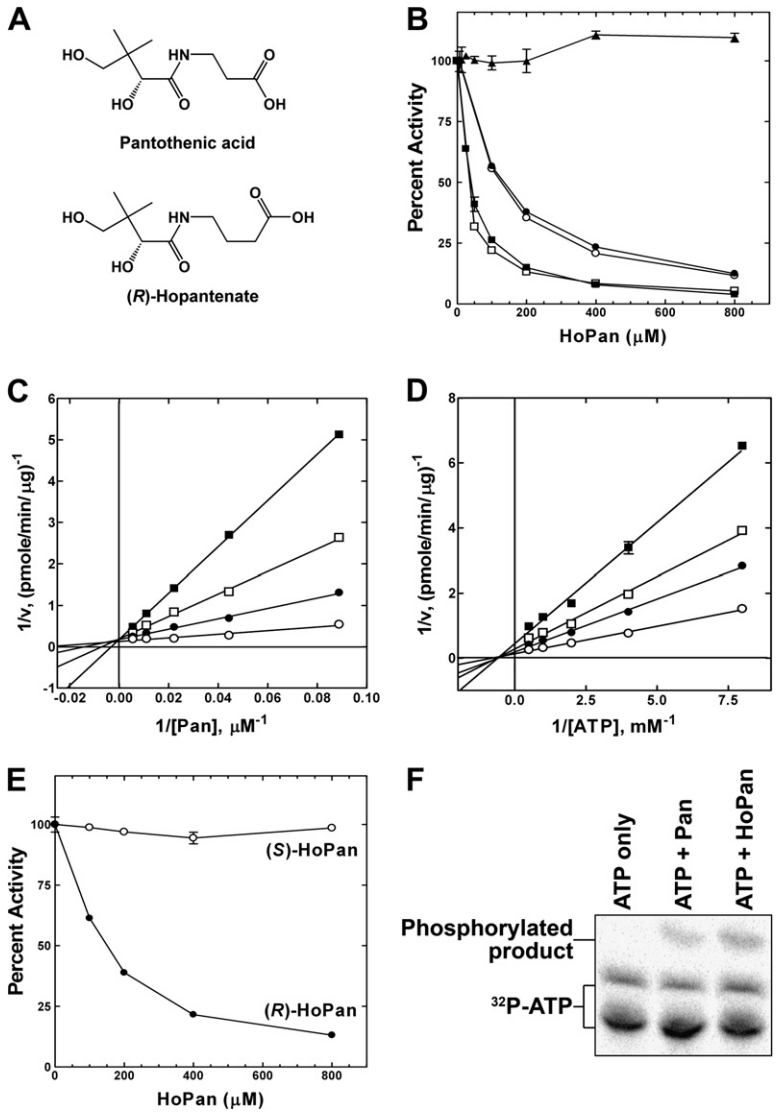

Figure 1. HoPan Inhibition of Pantothenate Kinase

(A) In HoPan (hopantenate), the β-alanine moiety of pantothenic acid is substituted with γ-aminobutyric acid (GABA), a neurotransmitter, that contains an additional methylene group.

(B) HoPan inhibited mouse PanK1α (●), PanK1β (○), PanK2 (■), and PanK3 (□) with IC_{50} values between 50 and 150 μM. The prokaryotic *E. coli* PanK (▲) was refractory to HoPan inhibition. Data presented are means with standard errors unless otherwise indicated.

(C and D) Kinetic analysis of the inhibition of PanK1α by HoPan illustrated that HoPan inhibition was competitive with pantothenate (C) and noncompetitive with respect to ATP (D). The mode of inhibition was determined at several HoPan concentrations: 300 μM (■), 150 μM (□), 75 μM (●), and 0 μM (○).

(E) (*R*)-HoPan (●) inhibited mPanK1α, but (*S*)-HoPan (○) was not active.

(F) PanK assays performed using [^{32}P]ATP showed that HoPan was phosphorylated by mPanK1α as well as the authentic pantothenate substrate. Products were detected by thin-layer chromatography as described in Experimental Procedures.

related structures [30]. The PanK1α, PanK1β, PanK2, and PanK3 proteins were expressed in 293T cells to evaluate their sensitivities to HoPan (see Figure S1 in the Supplemental Data available with this article online). The putative PanK4 was not enzymatically active when expressed in HEK293T cells (Figure S1). HoPan inhibited all active PanK isoforms with IC_{50}s between 50 μM and 150 μM in our in vitro assays (Figure 1B). Purified *Escherichia coli* PanK (CoaA), the prototypical type I pantothenate kinase, was refractory to inhibition (Figure 1B). HoPan inhibition of all the mammalian PanKs was consistent with the high degree of similarity among their catalytic domains [4, 6, 7, 12, 16]. Likewise, the PanK from *Aspergillus nidulans*, which belongs to the same PanK family as the mammalian isoforms [31], was inhibited by HoPan [30].

Analysis of the steady-state kinetics of the PanK reaction revealed competitive inhibition by HoPan with respect to the natural pantothenate substrate, as illustrated with PanK1α in Figure 1C. Lineweaver-Burk plots of 1/v versus 1/[ATP] demonstrated that HoPan was a noncompetitive inhibitor with respect to ATP (Figure 1D). The mode of inhibition was the same for PanK1β (Figure S2). Inhibition of PanK was stereoselective for the (*R*) isomer of HoPan (Figure 1E). We tested the reactivity of the inhibitor HoPan using [γ-^{32}P]ATP and PanK1α and detected phosphorylated HoPan formation (Figure 1F), revealing that HoPan was a pantothenate antimetabolite.

Physiological Effects of HoPan

HoPan was not toxic to cultured HEK293T, HepG2, or PC12 cells at concentrations up to 800 μM (Figure 2A). These experiments were performed in pantothenate-free Dulbecco's modified Eagle's medium (DMEM) supplemented with 1 μM pantothenate and dialyzed serum (up to 800:1 ratio of inhibitor to substrate). Consistent with its inhibitory effect on the PanKs in vitro, however, HoPan inhibited pantothenate incorporation into CoA in isolated primary hepatocytes, resulting in a blockade of CoA

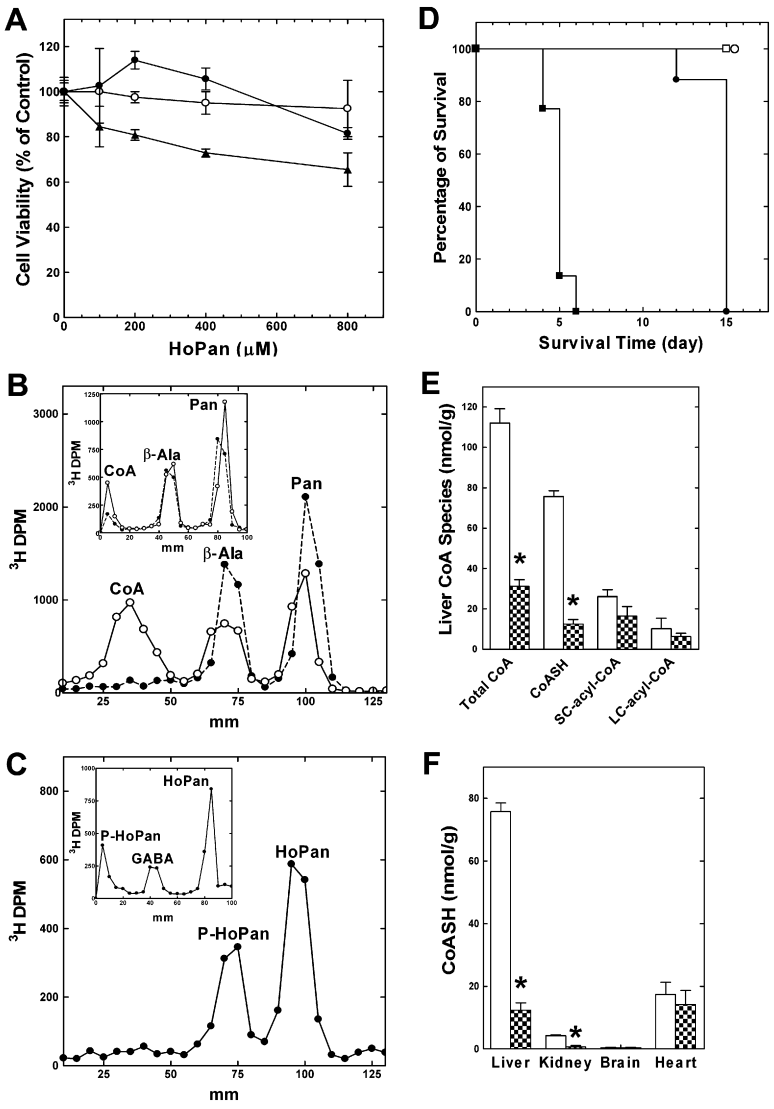

Figure 2. Toxicity of HoPan

(A) HoPan was not toxic to cultured cells. HepG2 (●), HEK293T (○), and PC12 (▲) cells were treated with HoPan at the indicated concentrations (800 μM, 400 μM, 200 μM, and 100 μM). Viable cells excluding trypan blue stain were counted after two doubling times. The number of viable cells is presented as the percentage of the control cells treated with dimethyl sulfoxide (vehicle alone).

(B) HoPan inhibition of CoA synthesis in isolated hepatocytes. Hepatocytes were isolated from male mouse liver and incubated with [^{3}H]pantothenate in the presence (●) and absence (○) of 5 μM HoPan. Hepatocytes were extracted and fractionated by thin-layer chromatography on silica gel H layers developed in solvent I (butanol:acetic acid:water, 5:2:3, v/v) and solvent II (ethanol:28% ammonium hydroxide, 4:1, v/v) (inset). Pan, pantothenate; β-Ala, β-alanine.

(C) HoPan was phosphorylated in vivo. Hepatocytes were labeled with [^{3}H]HoPan and the HoPan-derived intermediates were separated on thin-layer chromatography developed in solvent I and solvent II (inset). P-HoPan, phosphorylated HoPan.

(D) Survival of C57BL/6 mice (male, ■, n = 22, $p < 0.0001$; female, ●, n = 17, $p < 0.0001$) treated with HoPan (100 μg/g/day) compared to mice treated with an equal amount of HoPan plus pantothenate (male, □, n = 9; female, ○, n = 9).

(E and F) CoA levels in HoPan-treated (hatched bars) and control (open bars) mouse tissues. (E) shows the distribution of CoA species in male liver in control and HoPan-treated mice. HoPan treatment significantly reduced the levels of total CoA ($p < 0.0001$) and CoASH ($p < 0.0001$) in liver. (F) shows the CoASH levels in four representative mouse tissues. There was a significant drop of free CoA levels in liver and kidney ($p < 0.0001$), but not in brain or heart of HoPan-treated mice.

Error bars are standard errors of the mean.

production (Figure 2B). Hepatocytes labeled with [^{3}H]HoPan accumulated P-HoPan, demonstrating HoPan was phosphorylated in vivo and was not metabolized by the downstream enzymes of PanK (Figure 2C). The fact that no [^{3}H]Pan-derived intermediate accumulated in the HoPan-treated cells indicated that PanK was the only enzyme of CoA synthesis that was inhibited by HoPan treatment. Nonetheless, we tested the effects of HoPan and P-HoPan on the bifunctional CoA synthase in vitro. The results showed that neither compound inhibited the two activities of CoA synthase (data not shown). In contrast to immortalized cultured cells, animals rely heavily on oxidative metabolism, gluconeogenesis is critical for survival, and both processes depend on CoA. Thus, we administered HoPan to male and female mice (100 μg/g/day), all of which expired within 5 and 15 days, respectively (Figure 2D). Control male and female mice given HoPan plus an equal amount of pantothenate supplement survived the 16 day course of the experiment, demonstrating that the end result of HoPan treatment was specifically due to interference with pantothenate metabolism.

HoPan administration resulted in a precipitous decrease in liver total CoA levels, which were the highest among the four tissues examined and dropped by 73% (Figure 2E). Analysis of the distribution of CoA species showed that CoASH (nonesterified CoA) was the most significantly reduced in HoPan-treated liver. Kidney CoASH levels were lower than liver, but also exhibited a significant drop following HoPan (Figure 2F). Control male and female livers (HoPan + pantothenate) had between 110 and 125 nmol/g wet weight of CoA, which were the same as in mice maintained on chow without HoPan and regardless of pantothenate enrichment. The rapid CoA depletion in male liver implied that hepatic CoA had a high turnover rate compared to brain and heart. Assuming that CoA production was completely inhibited following the first dose of HoPan, the half-life for liver CoA was estimated to be 24–30 hr in male mice and ~90 hr in females. The different

turnover rates of CoA could account for the sexual dimorphism we observed in the HoPan-treated mice. In addition, possible different pharmacokinetics (absorption, excretion, and degradation of HoPan) in male and female mice could also explain the sexual dimorphism.

The livers from HoPan-treated mice exhibited distinct pathology characterized by marked vacuolization arising from swollen mitochondria (Figure 3). The liver sections stained with toluidine blue showed more lipid droplets, shrunken nuclei, and pronounced vacuoles in the cytoplasm in the HoPan-treated mice (Figures 3A and 3B). Transmission electron microscopy revealed that the apparent vacuoles were swollen mitochondria (Figures 3C–3F). Also, the glycogen storage granules evident in the control liver (Figure 3E) were missing from the HoPan-treated liver (Figure 3F). The brain, kidney, and heart exhibited normal histology in HoPan-treated male mice (not shown), pointing to the liver as the most sensitive target organ. All of the HoPan-treated animals also had elevated serum triglycerides, indicating defective utilization of this fuel source by the liver. Control sera from mice treated with HoPan plus Pan had 93 ± 47 mg/dl triglycerides, whereas sera from treated males had 230 ± 177 mg/dl ($p < 0.05$) (Table S1). The triglycerides in mice treated with H_2O vehicle was 76 ± 14 mg/dl (Table S1), similar to the level of the mice supplemented with pantothenate, demonstrating that pantothenate supplement completely countered the effect of HoPan. Serum triglycerides in female control mice increased from 55.3 ± 17.8 mg/dl in controls to 93.7 ± 78 mg/dl in HoPan-treated animals (Table S1). This increase was not statistically significant due to the variability in the data from the treated females.

Mechanism of HoPan Toxicity

Mice that succumbed to HoPan had low to undetectable (<20 mg/dl) glucose levels at or near the time they expired (Figure 4A), implicating hypoglycemia as a primary cause for death. A pyruvate tolerance test showed that the low blood glucose in the experimental animals was due to a defect in gluconeogenesis. Plasma glucose rose significantly in control animals following the injection of pyruvate; however, the HoPan-treated animals failed to convert the pyruvate into glucose (Figure 4B). Treated mice had lower levels of insulin (Figure 4C), and elevated levels of glucagon (Figure 4D) and corticosterone (Figure 4E), indicating a normal hormonal response to hypoglycemia [32]. These data indicated a metabolic imbalance in liver gluconeogenesis due to inadequate CoA rather than a hormonal deficiency. Also, HoPan moderately decreased lactate levels in both male (8.3 ± 1.6 to 5.7 ± 2.4 mmol/ml) and female (7.5 ± 3.8 to 5.3 ± 2.1 mmol/ml) mice (Table S1), arguing against lactic acidosis as a cause of death. We evaluated the response of female mice to fasting midway through the 2 week HoPan treatment program to investigate their ability to switch to fatty acids as a fuel source (Table S2). Animals treated with the antimetabolite had serum glucose (254.7 ± 79.7 mg/dl; n = 15) similar to controls (297.5 ± 52.8 ml/dl; n = 11), but were unable to maintain blood glucose during a 48 hr fast (61.1 ± 15.1 mg/dl; n = 31) and all 31 animals expired by 30 hr.

Alterations in Intermediary Metabolism and Gene Expression

The carnitine and organic acid compositions of HoPan-treated livers revealed several metabolic derangements created by reduced CoA (Figures 4F and 4G). Total acylcarnitines increased significantly. All but one of the acylcarnitine species were either increased or remained the same in HoPan-treated mice (Table S3) and the largest increases were in the levels of acetyl- and proprionylcarnitine. Free carnitine was also elevated, but not nearly to the same extent as the acylcarnitines (Table S3). Total organic acids did not appear to change in HoPan-treated mice due to the dominance of this pool by pyruvate. However, the second most abundant acid, lactate, decreased 50%, consistent with decreased serum lactate levels in HoPan-treated mice despite impaired gluconeogenesis. The tricarboxylic acid (TCA) cycle intermediates succinate, fumarate, and malate were all decreased (Figure 4G; Table S3). In addition, urea cycle intermediates ornithine and citrulline significantly accumulated in HoPan-treated mice (Figure 4G).

Microarray analysis showed that more than 3500 probe sets exhibited greater than 2-fold change with $p < 0.05$ in the HoPan-treated livers compared to the controls. A multiple hypothesis testing was performed and the q value was set at 0.05 to limit the false discovery rate to 5% [33, 34]. This analysis yielded 939 probe sets. Replicate probe sets representing the same genes were averaged to generate 772 unique probe sets, of which 502 had annotated biological processes indicating hepatic CoA depletion had a major effect on gene expression. Gene ontology analysis using the NetAffx Analysis Center [35] was carried out to obtain a global view of the hepatic genes affected by CoA depletion and correlate the significantly regulated probe sets with their biological functions. The most significantly perturbed physiological processes were lipid metabolism, organic acid/carboxylic acid metabolism, and protein metabolism (Figure 5). Among lipid metabolism genes, those responsible for biosynthesis were significantly repressed, whereas the expression of catabolic genes was elevated. For example, among the most highly induced genes were the acyl-CoA thioesterases (between 13- and 45-fold), whereas fatty acid synthase expression was reduced 5-fold (Table S4). Analysis of the array data by sorting gene ontology based on the subcellular location of the affected genes revealed that the proteins altered in the processes shown in Figure 5 were mainly associated with two membrane-bound organelles, the endoplasmic reticulum and mitochondria. This correlation arose from the association of many of the lipid metabolism genes with the endoplasmic reticulum, whereas the genes that affected organic acid metabolism are associated with the mitochondria.

A comparison between the gene expression array analyses and metabolic profiling of the HoPan-treated mouse livers revealed relationships between gene expression

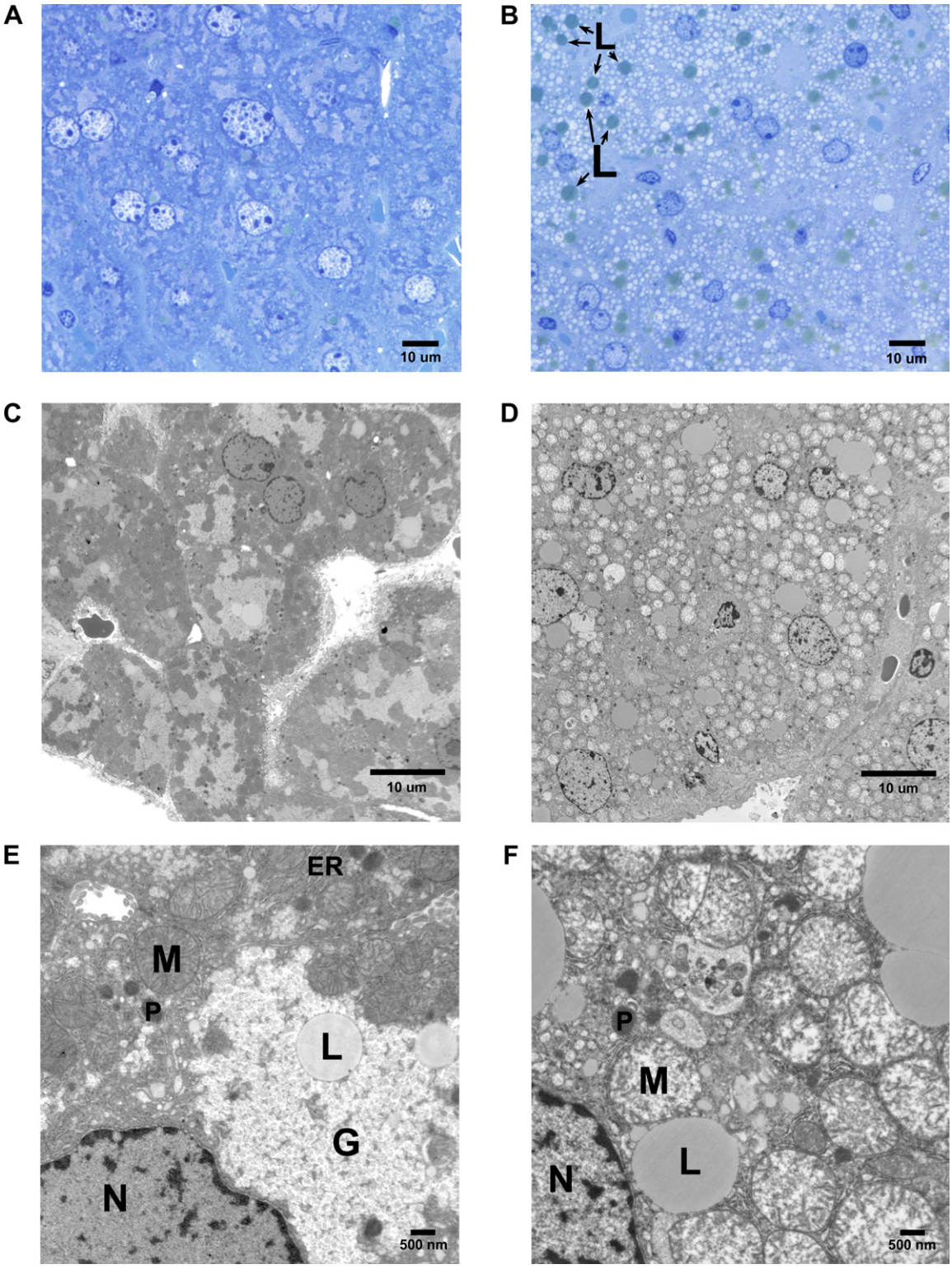

Figure 3. Liver Pathology in HoPan-Treated Mice

Liver sections from a control male mouse (A) and a HoPan-treated mouse (B) stained with toluidine blue. Transmission electron microscopy at two different magnifications of control male mouse liver (C and E) and HoPan-treated liver (D and F). L, lipid droplet; ER, endoplasmic reticulum; M, mitochondria; P, peroxisome; N, nucleus; G, glycogen storage granules.

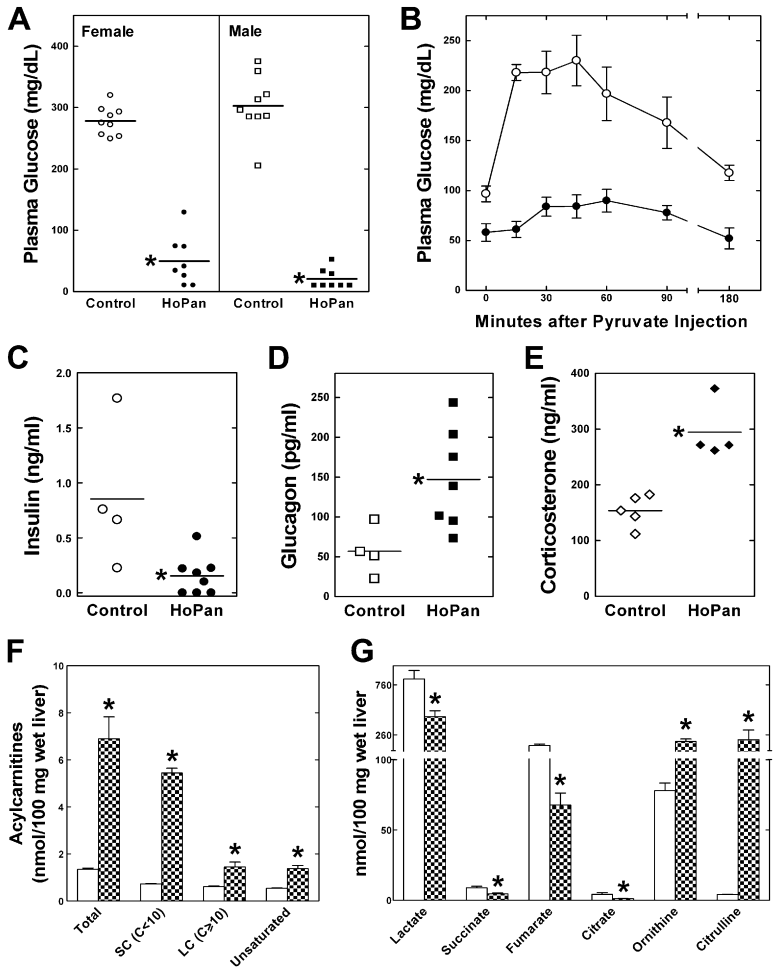

Figure 4. Metabolic Imbalances in HoPan-Treated Mice

(A) Plasma glucose levels of HoPan-treated mice (female, ●, n = 8, $p < 0.0001$; male, ■, n = 8, $p < 0.0001$) compared to mice treated with an equal amount of HoPan plus pantothenate (female, ○, n = 9; male, □, n = 9). Lines represent the means of each treatment group.

(B) Pyruvate tolerance test in mice (n = 5 per group) treated with HoPan (●) or water (○). Pyruvate injection significantly increased blood glucose levels in control mice in 15 min ($p < 0.0001$), whereas no significant increase was observed in HoPan-treated mice.

(C–E) Serum insulin (C), glucagon (D), and corticosterone (E) levels in HoPan-treated male mice. Closed symbols (●, ■, ◆) designate HoPan-treated mice and open symbols (○, □, ◇) designate the controls. The changes of serum insulin ($p = 0.014$), glucagon ($p = 0.026$), and corticosterone ($p = 0.0013$) levels in HoPan-treated mice were statistically significant.

(F and G) Alterations of liver acylcarnitines (F) and organic acids (G) in HoPan-treated mice. Asterisks indicate $p < 0.05$. A complete list of the panel of acylcarnitines and organic acids analyzed, their absolute tissue concentrations in the control and treated mice, and the statistical significance of the differences are found in Table S3. Open bars are the controls and hatched bars are the HoPan-treated mice. Error bars are standard errors of the mean.

(Table S4) and the perturbation in organic acid levels (Figure 4G). The reduced levels of the TCA cycle intermediates succinate and fumarate correlated with a 2.9-fold increase in expression of the downstream enzyme fumarate hydratase (*Fh1*). The microarray data also provided a basis for understanding the dysregulation of the urea cycle, exemplified by increased ornithine and citrulline intermediates following HoPan treatment. The expression of ornithine carbamoyltransferase (*Otc*), which utilizes ornithine, was depressed 8.5-fold and the expression of arginase (*Arg2*), which produces ornithine, increased 2.7-fold, consistent with the increased ornithine level (Figure 4G). The higher level of citrulline was linked to a 2.6-fold increase in the expression of the citrulline-forming enzyme nitric oxide synthase (*Nos3*). *PanK1* was the only pantothenate kinase gene that was upregulated (5.9-fold) in response to the blockade of CoA synthesis by HoPan, and none of the enzymes downstream of PanK in the CoA biosynthetic pathway was induced. Other biological processes that were affected by reduced CoA were the response to stress, development, and the immune response. A complete list of the genes significantly altered by HoPan treatment is presented in Table S4.

DISCUSSION

The metabolomic and gene expression analysis identified a program of adjustments focused on preserving the CoASH concentration (Figure 6). CoASH is required for several key mitochondrial reactions, including pyruvate dehydrogenase, α-ketoglutarate dehydrogenase, and fatty acid β-oxidation. The conversion of CoASH to acetyl-CoA from glycolysis via pyruvate is reduced by the 136-fold upregulation of pyruvate dehydrogenase kinase 1, which phosphorylates and inactivates pyruvate dehydrogenase. Acyl-CoA thioesterases 1, 2, and 3 are significantly upregulated (13- to 45-fold), illustrating a genetic adjustment to convert acyl-CoA to CoASH. Our metabolic profiling results provide experimental verification for the proposed role of carnitine as a sink to offload acyl moieties from acyl-CoA, thereby liberating CoASH to support cycling within mitochondria [36, 37]. The significant accumulation of acylcarnitines (5.1-fold) and the upregulation of carnitine palmitoyltransferase (4.7-fold) and carnitine acetyltransferase (2.7-fold) following HoPan administration are consistent with the function of carnitine in accepting acyl groups from acylated CoA and releasing CoASH to

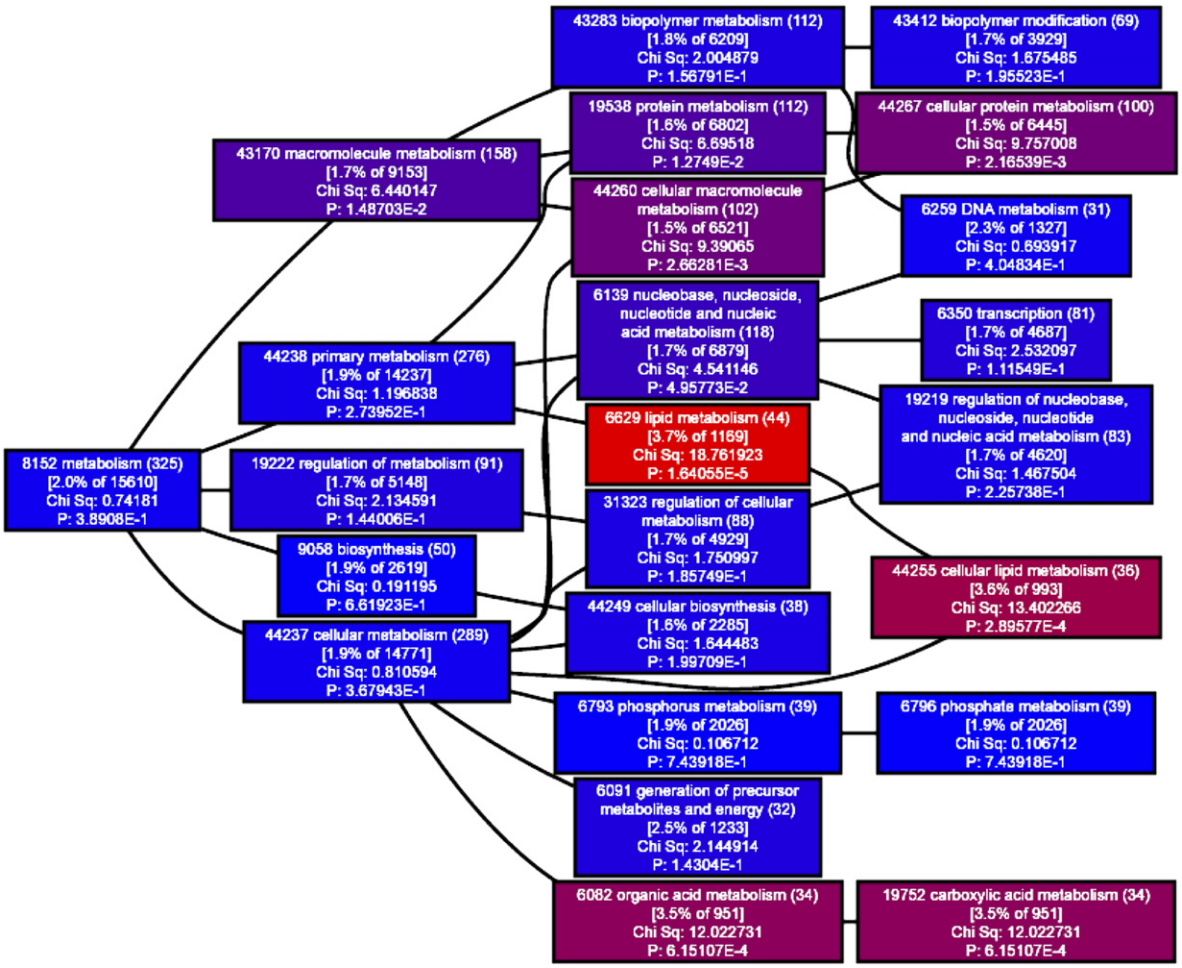

Figure 5. Gene Expression Alterations in HoPan-Treated Mice

The biological processes that correlated with the most significant changes in gene expression by HoPan treatment. Probe sets (772) that showed greater than 2-fold regulation, $p < 0.05$, and false discovery rate $q < 0.05$ were used in the gene ontology analysis. The graph was obtained using the NetAffx Analysis Center. Each box (node) represented one annotated biological process. The probe set count threshold for each node was set at 30. The color of the node was based on Chi square values: red indicates the most significant change, blue the least. A complete list of genes significantly regulated by HoPan treatment is presented in Table S4.

support gluconeogenesis and the urea cycle. The inability of HoPan-treated mice to produce glucose from liver and kidney is reflected by their inability to survive a brief fast and their failure in a pyruvate tolerance test. The impairment of gluconeogenesis and the accumulation of acylcarnitines in HoPan-treated mice are reminiscent of the phenotype of mouse models of fatty acid β-oxidation disorders. Acylcarnitines are formed within the mitochondria and released into the cytosol. Unlike CoA thioesters, acylcarnitines pass through biological membranes and are excreted in the urine, a diagnostic parameter for a number of inborn errors in mitochondrial function [38–40]. However, the HoPan phenotype differs in that animals with acyl-CoA dehydrogenase deficiencies accumulate serum lactate [38].

Our data show that liver actively controls the intracellular CoA concentration through a balance of synthesis and degradation. The synthetic arm of this regulatory cycle is governed by the four isoforms of pantothenate kinase, which are all expressed in liver. Each of these isoforms has a distinctive sensitivity to feedback inhibition by diverse CoA species [6, 7, 16], enabling the CoA biosynthetic flux to rapidly respond to branches of intermediary metabolism that differentially impact components of the CoA pool. Less is known about the genetic regulation of PanK expression, but the upregulation of hepatic PanK1α expression by fibrates [13] is an example of the modulation of gene expression levels by nutritional regulators. Adjustment of hepatic CoA levels in response to fasting or feeding conditions, diet, disease, or treatment with hypolipidemic drugs supports the importance of adjusting CoA levels in the metabolic adaptation of liver to different fuel sources [3, 10, 17–27]. Rapid turnover is a key feature of important metabolic regulatory cycles, and the abrupt cessation of CoA synthesis by HoPan leads to a precipitous decline in hepatic CoA levels as the degradative

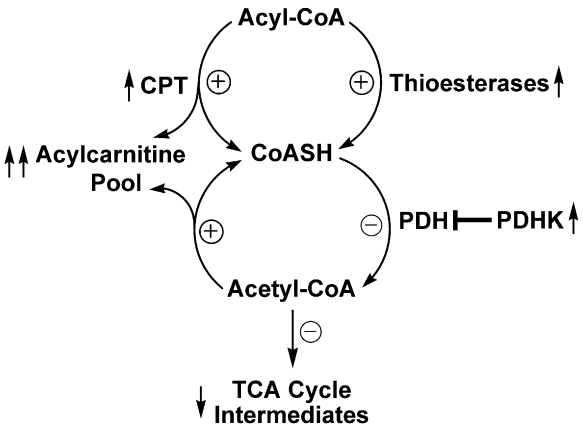

Figure 6. Mechanisms Buffering the Level of CoASH in Liver
Depletion of total hepatic CoA leads to a series of events that combine to spare the CoASH pool. The fall in acetyl-CoA leads to a decrease in mitochondrial energy generation via the TCA cycle reflected by the decrease in the concentration of 4-carbon organic acids participating in the cycle. CoASH conversion to acetyl-CoA is blocked both by the transfer of acetyl groups into the acetylcarnitine pool and the induction of pyruvate dehydrogenase kinase (PDHK) that phosphorylates and inactivates pyruvate dehydrogenase (PDH) shutting off glucose entry into the TCA cycle. Long-chain acyl-CoAs are removed by the elevated expression of thioesterases and carnitine palmitoyltransferase (CPT) that shuttles acyl moieties to the acylcarnitine pool.

branch of the regulatory cycle continues. Nudt7 is a peroxisomal protein that hydrolyzes CoASH and its thioesters [41]. Nudt7 is highly expressed in liver and kidney, in contrast to brain and heart [42], and this expression pattern correlates with liver and kidney exhibiting the most rapid decline in the total CoA pool in HoPan-treated animals, with the heart and brain being relatively unaffected (Figure 2F). Subcellular fractionation of mouse kidney showed that virtually all of the CoA hydrolase activity was associated with the peroxisomes, pointing to Nudt7 as the predominant enzyme responsible for CoA turnover [42]. The sexual dimorphism in the maintenance of hepatic CoA levels noted in this study may be due to differential expression of the pantothenate kinase isoforms in males and females, differences in the rates of CoA degradation, different pharmacokinetics toward HoPan, or a combination of these processes.

SIGNIFICANCE

CoA is a key cofactor in intermediary metabolism and its tissue levels are tightly regulated by the rate of biosynthesis at the pantothenate kinase step. This work integrates chemical genetics, metabolomics, and genomics to provide a comprehensive view of the abnormalities that arise from a defect in pantothenate kinase. Regulation of the CoASH pool is critical to support mitochondrial functions including gluconeogenesis, fatty acid oxidation, and the urea cycle. Multiple biochemical and genetic mechanisms are engaged to maintain CoASH. The carnitine transacylation systems play an important role in supporting CoASH levels by offloading acyl groups from acyl-CoAs. The alterations in intermediary metabolism in HoPan-treated animals serve as a model for the milder disruption of CoA homeostasis that underlies the abnormalities in pantothenate kinase-associated neurodegeneration (PKAN), a hereditary disorder arising from a deficiency in the mitochondrial PanK2 isozyme [12, 14].

These results also provide insight into understanding the toxicity of HoPan in humans. HoPan was originally developed as an antipsychotic drug to deliver the neurotransmitter γ-amino-iso-butyric acid to patients. HoPan showed some efficacy [43]; however, the side effects were so severe that therapy was discontinued. The adverse side effects induced hypoglycemia, hepatic steatosis, and organic acid excretion [44–48]. We attribute these side effects to the interference of HoPan with hepatic CoA metabolism, and our findings suggest that pantothenate supplementation would overcome these side effects, as it does in our mouse model.

EXPERIMENTAL PROCEDURES

Preparation of Pantothenate Kinases

Mouse PanK1α and PanK1β expression vectors were described previously along with the procedure for transfecting and assaying cell lysates [7]. The mouse cDNAs homologous to the human PanK2 and PanK3 proteins [12] were cloned into pcDNA3.1(−) (Invitrogen) and the human cDNA encoding PanK4 [12] was cloned with an amino-terminal His tag into pcDNA3.1/HisA (Invitrogen). Protein concentrations were determined by the method of Bradford [49] using γ-globulin as a standard. A peptide SKDNYKRVTGTSLGC was synthesized and coupled to keyhole limpet hemocyanin by the Hartwell Center for Biotechnology, St. Jude Children's Research Hospital, and was sent to Rockland, Inc. (Gilbertsville, PA) for raising rabbit polyclonal antiserum against PanK1, PanK2, and PanK3. Affinity-purified polyclonal antibody [7, 50] was used at a dilution of 1:500 (stock is 1.4 mg/ml) to detect proteins by western blot. The His-tagged human PanK4 protein was detected with anti-His rabbit IgG (Santa Cruz Biotechnology) used as the primary antibody at a dilution of 1:500 (stock is 0.2 mg/ml). Western blotting was used to confirm the expression of the PanK isoforms in the cell lysate as described [6].

Synthesis of HoPan

In two separate reaction vials, 4-aminobutyric acid (340 mg, 3.3 mmol) and diethylamine (345 μl, 3.3 mmol) were dissolved in methanol (10 ml). Then to the first reaction vial (*R*)-pantolactone (390 mg, 3 mmol) was added and to the second vial (*S*)-pantolactone (390 mg, 3 mmol) was added. The reactions were stirred overnight at 60°C, evaporated to dryness, and dissolved in 20 ml of water. Each mixture was passed through an Amberlite IR-120 (H^+) ion-exchange column (2 cm × 10 cm) and eluted with water until neutrality was obtained. These solutions were then washed three times with dichloromethane to remove any excess pantolactone. The extracted solutions were then evaporated to dryness to yield the (*R*)-4-(2,4-dihydroxy-3,3-dimethylbutylamido)butyric acid (**1**) and (*S*)-4-(2,4-dihydroxy-3,3-dimethylbutylamido)butyric acid (**2**) products, respectively, as oily residues which crystallized upon cooling. The Ca^{2+} salts of each product were obtained by dissolving each in 5 ml of methanol with the addition of 0.6 eq. of calcium hydroxide according to the protocol of Kopelevich et al. [51]. The solutions were gently warmed to 40°C and filtered to remove any

undissolved solid. The filtered solutions were evaporated to dryness to yield each product as a white amorphous powder.

Calcium (*R*)-4-(2,4-dihydroxy-3,3-dimethylbutylamido)butyrate (**1**) 406 mg (53% yield), a white powder; ^{1}H NMR (500 MHz, D_2O) δ 3.84 (s, 1H), 3.37 (d, *J* = 11.2 Hz, 1H), 3.25 (d, *J* = 11.2 Hz, 1H), 3.09 (t, *J* = 6.8 Hz, 2H), 2.07 (t, *J* = 7.8 Hz, 2H), 1.63 (qin, *J* = 7.3 Hz, 2H), 0.79 (s, 3H), 0.76 (s, 3H); MS (ESI^-) 231.9 (M − 1).

Calcium (*S*)-4-(2,4-dihydroxy-3,3-dimethylbutylamido)butyrate (**2**) 389 mg (51% yield), a white powder; ^{1}H NMR (500 MHz, CH_3OD) δ 3.95 (s, 1H), 3.49 (d, *J* = 11.0 Hz, 1H), 3.43 (d, *J* = 11.0 Hz, 1H), 3.28 (t, *J* = 6.8 Hz, 2H), 2.26 (t, *J* = 7.1 Hz, 2H), 1.82 (qin, *J* = 6.8 Hz, 2H), 0.97 (s, 3H), 0.95 (s, 3H); MS (ESI^-) 231.8 (M − 1).

Synthesis of [^{3}H]HoPan

To 4-amino-n-[2,3-^{3}H]butyric acid (1 mCi, 96.0 Ci/mmol) in 2% ethanol aq. (1 ml) was added cold 4-amino-butyric acid (1 mg, 10 μmol) in methanol (100 μl) and the mixture was concentrated to dryness in vacuo using a speedvac. The residue was resuspended in a solution of diethylamine (1.3 μl, 13 μmol) in methanol (100 μl) and to which was added (*R*)-pantolactone (1.7 mg, 13 μmol) in methanol (130 μl). The reaction mixture was heated overnight at 60°C and then concentrated to dryness. The resulting residue was resuspended in water (200 μl) and extracted with dichloromethane (200 μl) to remove any unreacted pantolactone. The aqueous phase was passed through a minicolumn of freshly activated Amberlite IR-120 (H^+) ion-exchange resin and the eluent was concentrated to dryness to afford [^{3}H]HoPan (4-(2,4-dihydroxy-3,3-dimethylbutylamido)-[2,3-^{3}H]butyric acid).

Pantothenate Kinase Assays

The standard pantothenate kinase assays were performed as described [7, 11]. HoPan phosphorylation was determined in a similar reaction mixture containing pantothenate (90 μM) or HoPan (400 μM), [γ-^{32}P]ATP (0.25 mM; specific activity 1 Ci/mmol; Amersham), $MgCl_2$ (10 mM), Tris-HCl (0.1 M, pH 7.5), and 40 μg of protein from a soluble PanK cell extract for a total volume of 40 μl. A 10 μl aliquot of the reaction mixture was spotted onto an activated silica gel H plate (Analtech) which was developed in butanol:acetic acid:H_2O (5:2:4, v/v/v), and the product was quantitated using ImageQuant (Molecular Dynamics).

HoPan Toxicity in Cell Cultures and Hepatocyte Labeling

HepG2 (American Type Culture Collection; ATCC), PC12 (ATCC), or HEK293T cells were cultured in pantothenate-free DMEM supplemented with 1 μM pantothenate and 10% dialyzed fetal bovine serum in the presence of various concentrations of HoPan. After two doubling times (48 hr for HepG2 cells, 30 hr for HEK293T cells, and 192 hr for PC12 cells), viable cells were counted, which excluded trypan blue.

Whole livers of two 4-month-old C57BL/6 male mice were harvested and rinsed in ice-cold buffer A (each liter contained 3.9 g of NaCl, 0.5 g of KCl, 24 g of HEPES, and 2.7 g of glucose; the pH was adjusted to 7.6). The liver was chopped with a Vibrotome tissue chopper at a setting of 0.5 mm and resuspended in 20 ml of erythrocyte buffer (15 ml of buffer A plus 5 ml of erythrocyte lysis buffer; Qiagen) in a 125 ml Erlenmeyer flask, gently mixed, and allowed to settle. The supernatant was carefully discarded, and the procedure with the erythrocyte buffer was repeated twice. The tissue pieces were then resuspended in 30 ml of digestion buffer (buffer A plus 0.7 g/l $CaCl_2$, 0.5 mg/ml type I collagenase, and 6 μg/ml deoxyribonuclease) and incubated in a water bath shaker at 37°C at 120 rpm for 20 min. The tissue pieces were allowed to settle on ice and the supernatant was transferred to a centrifuge tube. The tissue pieces were resuspended in another 30 ml of digestion buffer, the procedures were repeated twice, and the three supernatants were combined. Cell suspension from the supernatants was filtered through Spectra/Mesh nylon (41 μm; Fisher Scientific), and liver cells in the filtrate were centrifuged down at room temperature at 100 × g for 2 min. The cell pellet was resuspended in wash buffer (each liter contained 8 g of NaCl, 0.35 g of KCl, 0.16 g of $MgSO_4$, 0.18 g of $CaCl_2$, 2.4 g of HEPES, and 15 g of BSA; the pH was adjusted to 7.4) containing 10% erythrocyte lysis buffer (v/v) and centrifuged down three times.

Mouse liver cells were resuspended in PBS containing 0.5% BSA to the density of about 1 × 10^7 cells/ml. For each labeling experiment, 75 μl of the cell suspension was used. The cells were labeled with 2 μM [^{3}H]pantothenate (50 Ci/mmol) in the presence of 5 μM hopantenate or PBS (for control). For labeling with [^{3}H]HoPan (90 mCi/mmol, 400 μM), 500 μl of the cell suspension was used. After a 6 hr incubation at 37°C, cells were harvested and washed twice with PBS. The cells were lysed by sonication in 50 μl of lysis buffer (20 mM Tris-HCl [pH 7.5], 2 mM DTT, 5 mM EDTA, and 50 mM NaF). The identity of the intracellular metabolites was determined by fractionating the cell lysates by thin-layer chromatography on silica gel H plates developed in either solvent I (butanol:acetic acid:water, 5:2:3, v/v) or solvent II (ethanol:28% ammonium hydroxide, 4:1, v/v) using the standards described previously [2]. Sections (0.5 cm) were scraped from the plate and the radioactivity was quantitated in 3 ml of scintillation fluid using a liquid scintillation counter.

Animal Experiments

C57BL/6 mice (6 weeks old) were purchased from the Jackson Laboratory and fed on a diet without pantothenate supplement (TD 95248; Harlan) for 2 weeks prior to and during experimentation. Mice were maintained at a room temperature of 72° ± 2°F, room humidity of 50% ± 10%, and a 12 hr light, 12 hr dark cycle, with the dark cycle starting at 1800 hr. For time-to-death assays, calcium (*R*)-HoPan was dissolved in water and administered to 8-week-old mice daily by stomach gavage. Control mice were given water or HoPan plus an equal amount of pantothenate. In the fasting experiment, after 8-week-old female mice were administered HoPan at 100 μg/g/day by gavage for a week, one group of mice was fasted while the other group was fed as usual. HoPan was administered daily to both groups during the fasting period. Water was supplied ad libitum. Blood was drawn either by retro-orbital bleed or by cardiac puncture for glucose, lactate, and triglyceride tests performed by the Diagnostic Lab of the Animal Research Center, St. Jude Children's Research Hospital. Serum samples from HoPan-treated and control mice were sent to Ani Lytics, Inc. for insulin and glucagon measurements. Serum corticosterone levels were determined using the corticosterone enzyme immunoassay kit according to the manufacturer's instructions (Cayman Chemical). All procedures were performed according to St. Jude Children's Research Hospital Institutional Animal Care and Use Committee-approved protocols.

Pyruvate Tolerance Test

Female C57BL/6 mice (6 weeks old) were fed a low-pantothenate diet (TD 95248; Harlan) for 2 weeks prior to and during experimentation. Calcium (*R*)-HoPan (100 μg/g/day) or water was administered to the mice by stomach gavage. After 1 week of treatment, the pyruvate tolerance test was performed. The mice (five per group) were fasted for 14 hr before receiving an intraperitoneal dose of pyruvate (in saline) at 2 g/kg body weight. Plasma glucose levels were measured from the tail blood using a FreeStyle blood glucose monitoring system (TheraSense) at 0, 15, 30, 45, 60, 90, and 180 min after pyruvate infusion.

Measurement of CoA Species in Mouse Tissues

Extraction of different CoA species from mouse tissues and CoA assays were performed as described with modifications [52, 53]. Briefly, mouse tissue (0.1 g) was homogenized in 0.4 ml of chilled 6% perchloric acid containing 28 mM DTT. The precipitate containing the acid-insoluble long-chain acyl-CoAs, such as palmitoyl-CoA, was removed by centrifugation (1500 × g, 4°C, 10 min) and saved for long-chain acyl-CoA determination. Free CoA and short-chain acyl-CoAs, such as acetyl-CoA and malonyl-CoA, were acid soluble. The supernatant was split into two tubes, one for free CoA measurement, the other for both free and short-chain acyl-CoAs. For free CoA extraction, 0.1 volume of 1 M Tris and 0.3 volume of 2 M KOH were added before the pH was adjusted to 6.5∼8.5 with 0.6 N HCl

(and 200 mM KOH if necessary). The mixture was centrifuged (1500 × g, 4°C, 10 min) and the supernatant was saved for CoA determination. To extract free CoA and short-chain acyl-CoA from the other half of the supernatant, 1 M KOH was used to adjust the pH to 11∼12. The mixture was incubated at room temperature for 1 hr, neutralized with 0.6 N HCl to pH 6.5∼8.5, and centrifuged (1500 × g, 4°C, 10 min). The resultant supernatant was extracted with an equal volume of hexane three times before being used in the CoA determination assay. Long-chain acyl-CoAs were extracted from the initial perchloric acid precipitated pellet, which was washed with 0.6% perchloric acid containing 5 mM DTT and then washed with 5 mM DTT. The washed pellet was resuspended in 300 μl of 5 mM DTT and the pH was adjusted to 11∼12 with 1 M KOH. The mixture was incubated at room temperature for 1 hr, neutralized with 0.6 N HCl to pH 6.5∼8.5, and centrifuged (1500 × g, 4°C, 10 min). The resultant supernatant was extracted with an equal volume of hexane three times before being used in the CoA determination assay. The reaction mixture for the CoA measurement contained 200 mM Tris-HCl (pH 7.5), 8 mM $MgCl_2$, 0.1% Triton X-100, 2 mM EDTA, 20 mM NaF, 2.5 mM ATP, 10 μM [1-^{14}C]lauric acid, 100 ng of *E. coli* acyl-CoA synthetase (FadD), and tissue extract (5–20 μl) containing 25–400 pmol of CoA, in a total volume of 100 μl. The reaction was initiated by the addition of FadD, and the reaction mixture was incubated at 35°C for 30 min, followed by the addition of 325 μl of methanol:chloroform:n-heptane (1.41:1.25:1, v/v/v) and 25 μl of 0.4 M acetic acid. After the mixture was mixed vigorously and centrifuged, [1-^{14}C]lauroyl-CoA in the upper phase was quantitated by counting in 3 ml of ScintiSafe 30% using a Beckman LS 6500 scintillation counter. A standard curve using commercial CoA was used to calculate the amount of CoA species in mouse tissue extracts.

Metabolomic Profiling

Specimens of powdered liver tissue were homogenized in deionized water, and tissue extracts were prepared as previously described [54, 55]. Measurement of acylcarnitines, organic acids, and amino acids in tissue extracts was done by direct-injection electrospray tandem mass spectrometry, using a Quattro Micro LC-MS system (Waters-Micromass) equipped with a model HTS-PAL autosampler (Leap Technologies), a model 1100 HPLC solvent delivery system (Agilent Technologies), and a data system running MassLynx software.

Transcriptional Profiling

Total RNA was isolated using TRIzol (Invitrogen) according to the manufacturer's instructions. Pelleted RNA was resuspended in nuclease-free water and digested with DNase I to remove contaminating genomic DNA. The integrity of the total RNA was determined using the Agilent bioanalyzer Lab-on-a-Chip, and the RNA sample was converted to cDNA, labeled, and fragmented using procedures recommended by Affymetrix. Fragmented labeled cDNA (4.0 μg) was hybridized for 16 hr at 50°C to GeneChip mouse genome 430 2.0 arrays (Affymetrix). After washing, staining, and scanning of the arrays were performed according to the manufacturer's protocol (Affymetrix), the arrays were analyzed using GeneChip Operating Software (GCOS) and global scaling was used to normalize the data from different arrays. Spotfire DecisionSite 8.2.1 and the NetAffx Analysis Center [35] were used to analyze array results. The statistical analyses were from six data sets (three control and three HoPan-treated livers) that were independently processed and hybridized.

Statistical Analyses

The significance of HoPan treatment was determined using two-tailed, unpaired t tests with the confidence intervals set at 95%. Data with p values less than 0.05 are indicated with an asterisk in the figures.

Supplemental Data

Supplemental Data contain four tables and two figures and can be found with this article online at http://www.chembiol.com/cgi/content/full/14/3/291/DC1/.

ACKNOWLEDGMENTS

We thank Ruobing Zhou, Jina Wang, Pam Jackson, Daren Hemingway, Tuan Tran, Karen Miller, and Matthew Frank for their expert technical assistance. We also thank Sharon Frase and Lou Boykins of the Integrated Microscopy Center at the University of Memphis for their help with electron microscopy. This work was supported by National Institutes of Health grants GM45737 (S.J.), GM34496 (C.O.R.), and DK58398 (C.B.N.), Cancer Center (CORE) support grant CA21765, and the American Lebanese Syrian Associated Charities.

Received: September 11, 2006
Revised: December 20, 2006
Accepted: January 29, 2007
Published: March 23, 2007

REFERENCES

1. Leonardi, R., Zhang, Y.-M., Rock, C.O., and Jackowski, S. (2005). Coenzyme A: back in action. Prog. Lipid Res. *44*, 125–153.
2. Jackowski, S., and Rock, C.O. (1981). Regulation of coenzyme A biosynthesis. J. Bacteriol. *148*, 926–932.
3. Robishaw, J.D., Berkich, D.A., and Neely, J.R. (1982). Rate-limiting step and control of coenzyme A synthesis in cardiac muscle. J. Biol. Chem. *257*, 10967–10972.
4. Rock, C.O., Calder, R.B., Karim, M.A., and Jackowski, S. (2000). Pantothenate kinase regulation of the intracellular concentration of coenzyme A. J. Biol. Chem. *275*, 1377–1383.
5. Song, W.-J., and Jackowski, S. (1992). Cloning, sequencing, and expression of the pantothenate kinase (*coaA*) gene of *Escherichia coli*. J. Bacteriol. *174*, 6411–6417.
6. Zhang, Y.-M., Rock, C.O., and Jackowski, S. (2005). Feedback regulation of murine pantothenate kinase 3 by coenzyme A and coenzyme A thioesters. J. Biol. Chem. *280*, 32594–32601.
7. Rock, C.O., Karim, M.A., Zhang, Y.-M., and Jackowski, S. (2002). The murine *Pank1* gene encodes two differentially regulated pantothenate kinase isozymes. Gene *291*, 35–43.
8. Song, W.-J., and Jackowski, S. (1994). Kinetics and regulation of pantothenate kinase from *Escherichia coli*. J. Biol. Chem. *269*, 27051–27058.
9. Vallari, D.S., Jackowski, S., and Rock, C.O. (1987). Regulation of pantothenate kinase by coenzyme A and its thioesters. J. Biol. Chem. *262*, 2468–2471.
10. Halvorsen, O., and Skrede, S. (1982). Regulation of the biosynthesis of CoA at the level of pantothenate kinase. Eur. J. Biochem. *124*, 211–215.
11. Rock, C.O., Park, H.-W., and Jackowski, S. (2003). Role of feedback regulation of pantothenate kinase (CoaA) in the control of coenzyme A levels in *Escherichia coli*. J. Bacteriol. *185*, 3410–3415.
12. Zhou, B., Westaway, S.K., Levinson, B., Johnson, M.A., Gitschier, J., and Hayflick, S.J. (2001). A novel pantothenate kinase gene (*PANK2*) is defective in Hallervorden-Spatz syndrome. Nat. Genet. *28*, 345–349.
13. Ramaswamy, G., Karim, M.A., Murti, K.G., and Jackowski, S. (2004). PPARα controls the intracellular coenzyme A concentration via regulation of PANK1α gene expression. J. Lipid Res. *45*, 17–31.
14. Hörtnagel, K., Prokisch, H., and Meitinger, T. (2003). An isoform of hPANK2, deficient in pantothenate kinase-associated neurodegeneration, localizes to mitochondria. Hum. Mol. Genet. *12*, 321–327.
15. Ni, X., Ma, Y., Cheng, H., Jiang, M., Ying, K., Xie, Y., and Mao, Y. (2002). Cloning and characterization of a novel human pantothenate kinase gene. Int. J. Biochem. Cell Biol. *34*, 109–115.
16. Zhang, Y.-M., Rock, C.O., and Jackowski, S. (2006). Biochemical properties of human pantothenate kinase 2 isoforms and

mutations linked to pantothenate kinase-associated neurodegeneration. J. Biol. Chem. *281*, 107–114.

17. Voltti, H., Savolainen, M.J., Jauhonen, V.P., and Hassinen, I.E. (1979). Clofibrate-induced increase in coenzyme A concentration in rat tissues. Biochem. J. *182*, 95–102.
18. Smith, C.M., and Savage, C.R., Jr. (1980). Regulation of coenzyme A biosynthesis by glucagon and glucocorticoid in adult rat liver parenchymal cells. Biochem. J. *188*, 175–184.
19. Smith, C.M., Cano, M.L., and Potyraj, J. (1978). The relationship between metabolic state and total CoA content of rat liver and heart. J. Nutr. *108*, 854–862.
20. Kondrup, J., and Grunnet, N. (1973). The effect of acute and prolonged ethanol treatment on the contents of coenzyme A, carnitine and their derivatives in rat liver. Biochem. J. *132*, 373–379.
21. Lund, H., Stakkestad, J.A., and Skrede, S. (1986). Effects of thyroid state and fasting on the concentrations of CoA and malonyl-CoA in rat liver. Biochim. Biophys. Acta *876*, 685–687.
22. Savolainen, M.J., Jauhonen, V.P., and Hassinen, I.E. (1977). Effects of clofibrate on ethanol-induced modifications in liver and adipose tissue metabolism: role of hepatic redox state and hormonal mechanisms. Biochem. Pharmacol. *26*, 425–431.
23. Bhuiyan, A.K.M.J., Bartlett, K., Sherratt, H.S.A., and Agius, L. (1988). Effects of ciprofibrate and 2-[5-(4-chlorophenyl)pentyl]oxirane-2-carboxylate (POCA) on the distribution of carnitine and CoA and their acyl-esters and on enzyme activities in rats. Biochem. J. *253*, 337–343.
24. Skrede, S., and Halvorsen, O. (1979). Increased biosynthesis of CoA in the liver of rats treated with clofibrate. Eur. J. Biochem. *98*, 223–229.
25. Halvorsen, O. (1983). Effects of hypolipidemic drugs on hepatic CoA. Biochem. Pharmacol. *32*, 1126–1128.
26. Reibel, D.K., Wyse, B.W., Berkich, D.A., Palko, W.M., and Neely, J.R. (1981). Effects of diabetes and fasting on pantothenic acid metabolism in rats. Am. J. Physiol. *240*, E597–E601.
27. Reibel, D.K., Wyse, B.W., Berkich, D.A., and Neely, J.R. (1981). Regulation of coenzyme A synthesis in heart muscle: effects of diabetes and fasting. Am. J. Physiol. *240*, H606–H611.
28. Johnson, M.A., Kuo, Y.M., Westaway, S.K., Parker, S.M., Ching, K.H., Gitschier, J., and Hayflick, S.J. (2004). Mitochondrial localization of human PANK2 and hypotheses of secondary iron accumulation in pantothenate kinase-associated neurodegeneration. Ann. N Y Acad. Sci. *1012*, 282–298.
29. Kotzbauer, P.T., Truax, A.C., Trojanowski, J.Q., and Lee, V.M.Y. (2005). Altered neuronal mitochondrial coenzyme A synthesis in neurodegeneration with brain iron accumulation caused by abnormal processing, stability, and catalytic activity of mutant pantothenate kinase 2. J. Neurosci. *25*, 689–698.
30. Virga, K.G., Zhang, Y.-M., Leonardi, R., Ivey, R.A., Hevener, K., Park, H.-W., Jackowski, S., Rock, C.O., and Lee, R.E. (2006). Structure-activity relationships and enzyme inhibition of pantothenamide-type pantothenate kinase inhibitors. Bioorg. Med. Chem. *14*, 1007–1020.
31. Calder, R.B., Williams, R.S.B., Ramaswamy, G., Rock, C.O., Campbell, E., Unkles, S.E., Kinghorn, J.R., and Jackowski, S. (1999). Cloning and characterization of a eukaryotic pantothenate kinase gene (*panK*) from *Aspergillus nidulans*. J. Biol. Chem. *274*, 2014–2020.
32. Cryer, P.E. (1993). Glucose counterregulation: prevention and correction of hypoglycemia in humans. Am. J. Physiol. *264*, E149–E155.
33. Benjamini, Y., and Hochberg, Y. (1995). Controlling the false discovery rate: a practical and powerful approach to multiple testing. J. R. Stat. Soc. [Ser. B] *57*, 289–300.
34. Benjamini, Y., and Yekutieli, D. (2005). Quantitative trait loci analysis using the false discovery rate. Genetics *171*, 783–790.
35. Liu, G., Loraine, A.E., Shigeta, R., Cline, M., Cheng, J., Valmeekam, V., Sun, S., Kulp, D., and Siani-Rose, M.A. (2003). NetAffx: Affymetrix probesets and annotations. Nucleic Acids Res. *31*, 82–86.
36. Ramsay, R.R., and Zammit, V.A. (2004). Carnitine acyltransferases and their influence on CoA pools in health and disease. Mol. Aspects Med. *25*, 475–493.
37. Bieber, L.L. (1988). Carnitine. Annu. Rev. Biochem. *57*, 261–283.
38. Schuler, A.M., and Wood, P.A. (2002). Mouse models for disorders of mitochondrial fatty acid β-oxidation. ILAR J. *43*, 57–65.
39. Sim, K.G., Carpenter, K., Hammond, J., Christodoulou, J., and Wilcken, B. (2002). Acylcarnitine profiles in fibroblasts from patients with respiratory chain defects can resemble those from patients with mitochondrial fatty acid β-oxidation disorders. Metabolism *51*, 366–371.
40. Sim, K.G., Hammond, J., and Wilcken, B. (2002). Strategies for the diagnosis of mitochondrial fatty acid β-oxidation disorders. Clin. Chim. Acta *323*, 37–58.
41. Gasmi, L., and McLennan, A.G. (2001). The mouse *Nudt7* gene encodes a peroxisomal nudix hydrolase specific for coenzyme A and its derivatives. Biochem. J. *357*, 33–38.
42. Ofman, R., Speijer, D., Leen, R., and Wanders, R.J. (2006). Proteomic analysis of mouse kidney peroxisomes: identification of RP2p as a peroxisomal nudix hydrolase with acyl-CoA diphosphatase activity. Biochem. J. *393*, 537–543.
43. Task Force for Evaluation of Children's Behaviors (1974). A double-blind controlled study of Ca hopantenate and placebo in conformity to a rating list for the evaluation of the abnormal behaviors in children (III). Rinsho Hyoka *2*, 375–384.
44. Noda, S., Haratake, J., Sasaki, A., Ishii, N., Umezaki, H., and Horie, A. (1991). Acute encephalopathy with hepatic steatosis induced by pantothenic acid antagonist, calcium hopantenate, in dogs. Liver *11*, 134–142.
45. Ohsuga, S., Ohsuga, H., Takeoka, T., Ikeda, A., and Shinohara, Y. (1989). Metabolic acidosis and hypoglycemia during calcium hopantenate administration—report on 5 patients. Rinsho Shinkeigaku *29*, 741–746.
46. Nakanishi, T., Funahashi, S., Shimizu, A., and Hayashi, A. (1990). Urinary organic acids in elderly Japanese patients with ketosis and encephalopathy who have taken panto-yl-γ-aminobutyrate, calcium salt (calcium hopantenate, HOPA). Clin. Chim. Acta *188*, 85–90.
47. Matsumoto, M., Kuhara, T., Inoue, Y., Shinka, T., Matsumoto, I., and Kajita, M. (1990). Mass spectrometric identification of 2-hydroxydodecanedioic acid and its homologues in urine from patients with hopantenate therapy during clinical episode. Biomed. Environ. Mass Spectrom. *19*, 171–175.
48. Matsumoto, M., Kuhara, T., Inoue, Y., Shinka, T., and Matsumoto, I. (1991). Abnormal fatty acid metabolism in patients in hopantenate therapy during clinical episodes. J. Chromatogr. *562*, 139–145.
49. Bradford, M.M. (1976). A rapid and sensitive method for quantitation of microgram quantities of protein utilizing the principle of protein-dye binding. Anal. Biochem. *72*, 248–254.
50. Jackowski, S. (1994). Coordination of membrane phospholipid synthesis with the cell cycle. J. Biol. Chem. *269*, 3858–3867.
51. Kopelevich, V.M., Evdokimova, G.S., Marieva, T.D., and Shmuilovich, L.M. (1971). Synthesis of D-homopantothenic acid. Pharm. Chem. J. *5*, 534–536.
52. Rabier, D., Briand, P., Petit, F., Kamoun, P., and Cathelineau, L. (1983). Radioisotopic assay of picomolar amounts of coenzyme A. Anal. Biochem. *134*, 325–329.

53. Knights, K.M., and Drew, R. (1988). A radioisotopic assay of picomolar concentrations of coenzyme A in liver tissue. Anal. Biochem. *168*, 94–99.

54. Jensen, M.V., Joseph, J.W., Ilkayeva, O., Burgess, S., Lu, D., Ronnebaum, S.M., Odegaard, M., Becker, T.C., Sherry, A.D., and Newgard, C.B. (2006). Compensatory responses to pyruvate carboxylase suppression in islet β-cells: preservation of glucose-stimulated insulin secretion. J. Biol. Chem. *281*, 22342–22351.

55. An, J., Muoio, D.M., Shiota, M., Fujimoto, Y., Cline, G.W., Shulman, G.I., Koves, T.R., Stevens, R., Millington, D., and Newgard, C.B. (2004). Hepatic expression of malonyl-CoA decarboxylase reverses muscle, liver and whole-animal insulin resistance. Nat. Med. *10*, 268–274.

